# Fast, simple and calibration-free size characterization and quality control of extracellular vesicles using capillary Taylor dispersion analysis

Sameh Obeid, Joseph Chamieh, Thanh Duc Mai, Marco Morani, Melissa Reyre, Zuzana Krupova, Pierre Defrenaix, Hervé Cottet, Myriam Taverna

# Fast, simple and calibration-free size characterization and quality control of extracellular vesicles using capillary Taylor dispersion analysis

Sameh Obeid[a], Joseph Chamieh[b], Thanh Duc Mai[a], Marco Morani[a], Melissa Reyre[c], Zuzana Krupova[c], Pierre Defrenaix[c], Hervé Cottet[b], Myriam Taverna[a,*]

[a]Université Paris-Saclay, CNRS, Institut Galien Paris-Saclay, 91400, Orsay, France

[b]IBMM, Université de Montpellier, CNRS, ENSCM, Montpellier, France

[c]Excilone - 6, Rue Blaise Pascal - Parc Euclide, 78990, Elancourt, France

***Corresponding author.**

**E-mail address:** myriam.taverna@universite-paris-saclay.fr

**Abstract**

This study reports the development of a Taylor Dispersion Analysis (TDA) method for the size characterization of Extracellular Vesicles (EVs), which are highly heterogeneous nanoscale cell-derived vesicles (30-1000 nm). Here, we showed that TDA, conducted in uncoated fused silica capillary (50 µm i.d.) using a conventional Capillary Electrophoresis instrument, is able to provide absolute sizing (requiring no calibration) of bovine milk-derived EVs in a small sample volume (~ 7 nL) and over their entire size range, even the smallest ones (< 70 nm) not accessible via other techniques that provide nanoparticle sizing in suspension. TDA size measurements were repeatable (RSD < 10%) and the average EV sizes were found in the range of 120-210 nm, in very good agreement with those measured with Nanoparticle Tracking Analysis, commonly used for EV characterization. TDA allowed quantitative estimation of EVs for concentrations ≥ $2x10^{11}$ EVs/mL. Furthermore, TDA was able to detect minor changes in EV size (i.e. by ~25 nm upon interaction with specific anti-CD9 antibodies of ~150 kDa), and to highlight the impact of extraction methods (i.e. milk pretreatment: freezing, acid precipitation or centrifugation; the type of size-exclusion chromatography column) and of fluorescent labeling (i.e. intravesicular or surface labeling) on the isolated EV population size. In parallel to EV sizing, TDA allowed to detect molecular contaminants (average sizes ~1-13 nm) present within the sample, rendering this method a valuable tool to assess the quality and quantity of EV isolates.

***Keywords:*** *Taylor Dispersion Analysis, Extracellular Vesicles, Size characterization, Quality control, Capillary Electrophoresis*

## 1. Introduction

Extracellular Vesicles (EVs) are a heterogeneous group of cell-derived membrane-bound vesicles, with sizes ranging between 30-1000 nm (typically <500 nm), released by both eukaryotic and prokaryotic cells [1–3]. EVs are currently classified into three major groups based on their biogenesis mode: Exosomes, microvesicles and apoptotic bodies. Unlike apoptotic bodies, exosomes and microvesicles are secreted by healthy cells. However, due to the difficulties in assigning an EV to a particular biogenesis pathway, the generic term EVs is now widely used for all lipid bilayer-delimited particles and naturally released from cells [4]. EVs play a crucial role in intercellular communication as they facilitate the transfer of proteins, lipids and nucleic acids between cells under physiological and pathological conditions. Over the past decade, the interest in studying EVs has been growing since these vesicles are regarded as promising diagnostic and prognostic biomarkers as well as new therapeutic agents or drug delivery nanosystems [3,5,6].

A variety of well-established techniques and approaches are being commonly used for the detection and characterization of EVs, including microscopic methods (e.g. electron microscopy, atomic force microscopy), dynamic light scattering (DLS), nanoparticle tracking analysis (NTA), tunable resistive pulse sensing (TRPS) and flow cytometry [7–9]. Novel analytical methods are also being developed and optimized to study EVs such as imaging flow cytometry, interferometric plasmonic imaging and various microfluidic-based technologies [10,11]. However, the accurate assessment of nanometric EVs is hampered by technical challenges related to EV's inherent properties [12], notably their high degree of heterogeneity in biochemical composition due to different cellular origin and their complex biogenesis [3]. Furthermore, the contaminants present in EV samples (e.g. protein complexes/aggregates and lipoproteins), which may overlap in size, density and/or compositions with EVs, often interfere with their functional and physical characterization [13]. This comes from the fact that currently used isolation methods, which affect directly the yields, purity and type of isolated EVs, lack standardization [7,14]. Due to these challenges, the methods used for EV characterization are still limited in terms of size detection range, accuracy, sampling representativeness and/or reproducibility. This is further complicated by the lack of reference materials that can be reliably used to calibrate EV analysis techniques (e.g. optical techniques such as flow cytometry and NTA) and standardize measurements between labs [15,16]. Thus, powerful techniques allowing rapid and accurate physical characterization and particularly

sizing of EVs in suspension, over their entire size range, with minimal sample consumption and calibration requirements, are still in great demand.

Here, we propose a new alternative technique for the sizing of EVs and the assessment of their purity using Taylor Dispersion Analysis (TDA). This technique, which is based on Poiseuille laminar flow-induced dispersion [17], is a simple and rapid method for the determination of the weight-/number- averaged hydrodynamic radii. It is also an absolute method requiring no calibration nor prior knowledge of the sample concentration. TDA is applicable to any kind of analyte of virtually any size ranging from angstrom to sub-micrometer, with much less bias from the presence of large particles or aggregates compared to DLS [18]. In addition, any kind of sample matrix or medium can be employed for this analysis. The elution profile of the analytes can be detected using various detection modes such as UV absorbance, fluorescence, Inductively Coupled Plasma-Mass Spectrometry (ICP-MS), backscattering interferometry and photochemical oxidation [18–21]. These features make TDA a promising tool for studying heterogeneous (in size and composition) particles such as EVs. Furthermore, TDA can be conducted in narrow fused silica capillaries (*typically* ~50 µm i.d.) and using a conventional Capillary Electrophoresis (CE) instrument, presenting several advantages such as a very small sample volume consumption (i.e. ~10 nL per injection) and a high degree of automation. While TDA has been applied to a broad range of analytes from small molecules [22,23] to nano-scale particles of various sizes up to 250 nm [24–28], to date, determining the diffusion coefficients of EVs by TDA, and thus their mean hydrodynamic size, has never been explored.

Herein, we optimized TDA conditions coupled to UV and laser-induced fluorescent (LIF) detection to investigate the size of bovine milk-derived EVs using fused silica capillaries. TDA measurement sensitivity and accuracy were also evaluated. The developed TDA-UV method was employed to explore the impact of milk pretreatments and isolation methods on the size and purity of the isolated EVs. In parallel, we evaluated the efficacy of TDA coupled to LIF detection to provide specific sizing of EVs after labeling with an intravesicular fluorescent dye (i.e. CFDA-SE) or FITC-conjugated antibody directed against an EV membrane tetraspanin. This work demonstrates the potential of TDA for the size characterization and quality assessment of EVs, while providing also quantitative estimation of isolated EVs.

## 2. Materials and methods

### 2.1. Chemical and reagents

Dulbecco's phosphate buffered saline (PBS), sodium dodecyl sulfate (SDS, 98.5% (GC)) and Protease Inhibitors Cocktail (cOmplete™, Mini, Roche) were purchased from Merck (Saint Quentin Fallavier, France). Sodium hydroxide (NaOH, 1M) was obtained from VWR (Fontenay-sous-Bois, France). Buffers were prepared with deionized water purified with a Direct - Q3 UV purification system (Millipore, Milford, MA, USA). Coomassie (Bradford) Protein Assay Kit, Bovine Serum Albumin (BSA), Vybrant™ CFDA-SE Cell Tracer Kit (dye 5-(and-6)-Carboxyfluorescein diacetate succinimidyl ester), unconjugated- and FITC-conjugated mouse anti-bovine CD9 monoclonal antibodies (MM2/57) were purchased from ThermoFisher Scientific (Illkrich, France). EV samples were isolated from bovine milk or whey protein concentrate (WPC), using different protocols described below. The WPC samples were kindly provided by the Dairy Goat Co-operative (N.Z.) (DGC, Ltd, Hamilton New Zealand).

## 2.2. Isolation of EVs from fresh and frozen bovine milk

EVs were prepared from fresh bovine milk samples (BM), or frozen BM (f-BM) in the presence of proteases inhibitors. Whole bovine milk samples (50 mL) were centrifuged at 3000 xg for 30 min at 4°C (Allegra X-15R, Beckman Coulter, France) to separate fat globules, cells and cell debris from skimmed milk. The major milk proteins (i.e. caseins) were subsequently discarded from skimmed milk either by acid precipitation (AP) or by *centrifugation (C)* prior to EV isolation from the whey portion of milk using size exclusion chromatography.

### 2.2.1. Preparation of whey by acid precipitation of major milk proteins (caseins)

Acid precipitation of major milk proteins was done by adding 10 % acetic acid to the milk samples and by incubation at 37°C for 10 min and then continued by addition of 5 mL of 1M sodium acetate, and incubation for 10 min at RT. This was followed by centrifugation at 1500 xg, 4°C for 15 min and filtration of supernatant using vacuum-driven filtration system Millipore Steritop, 0.22 µm. The whey supernatants were concentrated by centrifugation at 4000 xg and 20°C using Amicon 100 kDa centrifugal filter units (Merck Millipore).

### 2.2.2. Preparation of whey by pelleting of major milk proteins (caseins) by centrifugation

Whey was prepared using two different centrifugation protocols. Briefly, the initial volume of 45 mL of skimmed milk was distributed in 1 and 2 mL alliquots. One or two milliliters of

skimmed bovine milk were centrifugated at a mid-force of 21,500 xg for 35 min (protocol C1) or 50 min (protocol C2), at 4°C, respectively. Sequential filtration of both whey preparations using 0.45 & 0.22 µm membranes (Sartorius Minisart) was performed prior to concentration step by Amicon-15 100 kDa filter units up to 6 mL of final volume (Merck Millipore).

#### 2.2.3. Isolation of EVs from whey using size exclusion chromatography (SEC)

Five hundred µl of a whey sample, obtained from fresh or frozen BM by acid precipitation (BM-AP or f-BM-AP), or from frozen milk by centrifugation (f-BM-C), was loaded onto a qEV original SEC 70 nm (qEV70) or qEV original SEC 35 nm (qEV35) columns (Izon Science, New Zealand), previously washed and equilibrated with PBS, and EV populations were fractionated. Fraction collection (0.4 mL per fraction) was carried out immediately using PBS as the elution buffer. The selected elution fractions (1-3) were pooled. Several washing steps with PBS were applied to obtain highly pure EV fractions and were subsequently concentrated using 100 kDa Amicon centrifugal filter units (Merck Millipore).

### 2.3. Isolation of EVs from bovine whey protein concentrate (WPC)

WPC was spray dried, soluble milk protein manufactured from fresh New Zealand cheese whey using an ultra-filtration process. The protein content of WPC was 80.3 g of total whey proteins per 100 g of dried powder. Bovine WPC was reconstituted in triplicate according to instructions of Dairy Goat Cooperative (DGC). Briefly, 10 grams of whey protein concentrate was resolved in 100 mL of warm water (30 °C). The final volume of 20 ml of reconstituted whey was used for pre-treatment stage. The same methodology for pre-treatment by acid precipitation and EV isolation was used as described previously for isolation of EVs from the whey fraction of bovine milk using SEC approach, except the loaded volume. After acid precipitation of the milk samples, 100 µl of pre-treated whey was loaded onto a qEV original SEC 70 column (Izon Science, New Zealand) previously washed and equilibrated with PBS and EV populations were fractionated. Fraction collection (0.5 mL per fraction) was carried out immediately using PBS as elution buffer. The selected elution fractions were pooled as described previously (Section 2.2.3) and were subsequently concentrated using 100 kDa Amicon centrifugal filter units (Merck Millipore).

### 2.4. Characterization of EV preparations

To validate the preparations of enriched EVs from BM or WPC, the absence of EVs in the eluents and filtrates was verified, serving to control the purification efficiency. Once the

purification was completed, the isolated populations were characterized by Bradford assay, by Transmission Electron Microscopy (TEM), with negative staining by uranyl acetate, and by Nanoparticle Tracking Analysis (NTA).

#### 2.4.1. EV protein concentration determination

One microliter of each EV sample was used to measure the protein concentration by Bradford assay. A standard linear curve was set up using BSA. Measurements were done in triplicate.

#### 2.4.2. Nanoparticle tracking analysis of EVs

EV size distribution and particle concentration were determined with NTA Zetaview (Particle Metrix, Germany) system. All experiments were carried out with pre-diluted samples in PBS, leading to particle concentration within the $10^7$-$10^9$ particles/mL range for optimal analysis. The Zetaview system (Particle Metrix) is equipped with a 488 nm laser. NTA analysis was performed in triplicate for each sample. Each measurement was performed on 11 different positions within the sample cell with following specifications and analysis parameters: sensitivity 80, shutter 100, Max Area 1000, Min Area 10, Min Brightness 20. The results were validated while obtaining at least 1000 valid tracks for each run. For data capture and analysis, the NTA software version 8.05.05 SP2 (Particle Metrix) was used. Data represent the mean size $\pm$ standard deviation (SD) of triplicate measurements.

#### 2.4.3. Transmission electron microscopy (TEM) of EV isolates

The EVs were analyzed after deposition of 4 µl of suspension on a copper grid covered with a carbon film for 5 mins, then stained with 1% uranyl acetate after absorption of the contrasting liquid excess. The grids were observed on a Hitachi HT7700 transmission electron microscope at 80 kV (Elexience - France). Images were acquired using an AMT camera.

### 2.5. Taylor Dispersion Analysis of EVs

The TDA-UV and TDA-LIF experiments were carried out using Sciex MDQ CE systems (Sciex Separation, Brea, CA) equipped either with UV absorption detector (200nm) or a solid-state laser induced fluorescence detector ($\lambda_{excitation}$: 488 nm, $\lambda_{emission}$: 520 nm) positioned at 50.2 cm from the inlet of the capillary. The TDA-UV and TDA-LIF measurements were performed at 20°C and 25°C, respectively. Uncoated fused silica capillaries (CM Scientific, Silsden, UK)

with I.D. of 50 µm, O.D. of 375 mm, effective length ($L_{eff}$) of 50.2 cm and total length ($L_{tot}$) of 60 cm were used. The capillaries were preconditioned by successive flushing at 1.4 bar with water for 10 min, 1 M NaOH for 10 min and then water for 10 min. The EV samples were injected hydrodynamically from the inlet end by applying a pressure of 28 mbar for 9 s, corresponding to a volume of ~7 nL. The mobilization pressure was kept constant at 28 mbar. PBS 1X was used as the mobilization buffer. The injected EV concentrations were estimated based on NTA. All EV samples were diluted in PBS 1X at the desired concentration prior to their analysis. The measurements were performed in triplicate. Taylorgrams were recorded using Karat 32 software and then exported into an Excel file for subsequent data processing, where the temporal variance of the elution profile was quantified by peak integration. The latter is the result of the peak broadening due to Taylor dispersion. Consequently, the diffusion coefficient $D$ ($m^2\ s^{-1}$) and the hydrodynamic radius $R_h$ (m) are determined using Eq. (1) and Eq. (2), respectively:

$$D = \frac{R_c^2 t_0}{24\sigma^2} \quad (1)$$

$$R_h = \frac{k_b T}{6\pi\eta D} \quad (2)$$

where $R_c$ is the capillary radius (m), $t_0$ is the average elution time (s), $\sigma^2$ is the temporal variance of the peak ($s^2$), $k_B$ is the Boltzmann constant ($J\ K^{-1}$), $T$ the temperature (K) and $\eta$ the viscosity of the carrier liquid (Pa s). It is noteworthy that Eq. (1) is valid when the peak appearance time $t_0$ is higher than the characteristic diffusion time of the solute on a distance equal to the capillary radius as verified by Eq. (3) [29,30]:

$$\tau = \frac{D t_0}{R_c^2} \geq 1.25 \quad (3)$$

where $\tau$ is an adimensional characteristic time. Axial diffusion should also be negligible compared to convection as verified by Eq. (4) [29,30]:

$$P_e = \frac{u R_c}{D} \geq 40 \quad (4)$$

where $P_e$ is the Peclet number and $u$ is the linear mobile phase velocity (m/s).

In the case of a sample mixture containing $n$ different components of individual diffusion coefficient $D_i$, the Taylorgram $S(t)$ can be expressed as a sum of $n$ individual Gaussian contributions $S_i(t)$, all centered at the same elution time $t_0$:

$$S(t) = \sum_{i=1}^{n} S_i\ (t) = \sum_{i=1}^{n} \frac{A_i}{\sigma_i \sqrt{2\pi}} e^{-\frac{1(t-t0)^2}{2\ \sigma_i^2}} \quad (5)$$

where $A_i$ is a coefficient that is proportional to the concentration in species *i* and that depends on the response coefficient of the species *i,* at the specific detection wavelength. The diffusion coefficient of the species *i* is directly related to the standard deviation $\sigma_i$ according to equation (1). In order to obtain information about the size distribution of the species in the mixture from the Taylorgram *S(t)* a direct curve fitting of the elution profile with the sum of *n* Gaussian curves according to equation (5), was applied when the total number of species, *n,* is limited ($n \leq 4$). The curve fitting was conducted using the Least Significant Difference method and the "GRG nonlinear" algorithm in Microsoft Excel. The *n*-Gaussian fit was performed only on the left half of the elution peak to avoid any impact of eventual peak tailing on the size measurement. Repeatability of TDA measurements was quantified by calculating the relative standard deviation (RSD) on $R_h$ values. The data represent mean size $\pm$ SD.

## 2.6. Labeling of EVs

### 2.6.1. With antibodies

For labeling of EVs with a specific antibody directed against CD9 tetraspanin, 10 µL of EVs (at $2x10^{12}$ EVs/mL) were incubated with the anti-CD9 monoclonal antibody (MM2/57), at a final concentration of 2 µg/mL, for 1 h at RT. Labeling EVs with anti-CD9 conjugated to FITC was done by incubation of EVs with the fluorescent antibody (final concentration of 4 µg/mL), for 1 h at RT. Fluorescently labeled EVs were then washed twice with PBS, to remove free antibodies, by centrifugation at 10 000 xg using a Nanosep centrifugal tube with 300K MWCO Omega™ membrane (Pall laboratory). The estimation of the final labeled EV concentrations was based on the initial EV concentrations (i.e. before labeling), determined by NTA, and taking into account the final volume recovered after the washing steps.

### 2.6.2. With a fluorescent dye

The fluorescent labeling of EVs was implemented using the 5-(and-6)-Carboxyfluorescein diacetate succinimidyl ester (CFDA-SE) dye according to the protocol described previously [31]. Briefly, a 10 mM stock solution of the dye was first prepared in DMSO following the manufacturer's instructions. Prior to the labeling, the DMSO stock solution was diluted to 200 µM in PBS. EVs were incubated with CFDA-SE (50:50, v/v) for 2 h in the dark, at RT.

Labeled EVs were then washed twice with PBS, to remove residual free CFDA-SE, by centrifugation at 12000 x g using a Microcon-30 kDa centrifugal filter unit (Millipore).

### 2.7. Statistical analysis

Data were analyzed with GraphPad Prism 9 (CA, USA). Unpaired two-tailed Student's t-test was used to compare two different samples measured by the same technique (TDA or NTA) and results obtained for the same sample by both techniques. Moreover, one-way ANOVA with Tukey's multiple-comparison test was used to evaluate whether the mean EV size, determined by TDA, changes as function of the injected concentration. Data were considered significantly different at $p$ value ≤ 0.05 (> 0.05 equals not significant (ns), ≤ 0.05 *, ≤ 0.01 **, ≤ 0.001 ***).

## 3. Results and discussion

### 3.1. Optimization and validation of TDA method for measurement of EV sizes and concentrations

Operating conditions in TDA (mobilization pressure, capillary nature and dimensions) were carefully selected to remain in the Taylor regime (i.e. equations (3) and (4) were fulfilled), for all solutes having a hydrodynamic diameter ($D_h$) ranging from 1 to about 300 nm (Chamieh et al., 2017). TDA-UV was first conducted on EVs isolated from fresh bovine Milk (BM), which was pretreated by acid precipitation and purified using a qEV35 SEC column (BM-AP-qEV35). The selected mobilization buffer was 1x PBS and all analyzed samples were diluted also in that buffer. The elution peak appeared relatively symmetric indicating minimal adsorption of analytes onto the silica capillary wall under those conditions (Fig. 1-A). The peak was best fitted with the sum of two Gaussians due to the presence of UV absorbing small molecules within the EV sample, appearing as a small peak at the top of the UV signal. The major population, contributing to 94 ± 1 % of the total UV absorbance signal, represents EVs and was shown to exhibit an average hydrodynamic diameter of 189.9 ± 5.4 nm. This value is in good agreement with the results obtained by NTA for this sample, which indicated an average EV size of 178.7 ± 6.7 nm (Fig. 1-B, Table 1). The smallest size population revealed with TDA showed a mean size of 1.22 ± 0.04 nm and represented only 6 ± 1 % of the total UV signal. This population is probably constituted by residual small contaminants co-isolated with EVs, such as β-lactoglobulin, the main whey protein with a hydrodynamic size of ~1.2 nm [32], which was particularly found to be present in BM-derived EV samples prepared by acid precipitation when analyzed by mass spectrometry (data not shown). Hence, in addition to EV size characterization, TDA offers

the advantage to detect the presence of molecular contaminants within the sample, which are below the size limit of NTA of 70 nm [33].

To assess the performance of TDA-UV for measurement of EV size and concentrations, the experiments were performed with EVs at different concentrations (from $2\times10^{11}$ to $2\times10^{13}$ EVs/mL) and with triplicate analyses. Size measurements were highly repeatable for EV concentrations over $5\times10^{11}$ EVs/mL, with RSD ranging from 2.4 to 7.6% (Fig. 1-A, C). Moreover, the average EV size measured by TDA was similar (~191 nm; $p>0.05$) regardless of the injected EV concentration (Fig. 1-C). The TDA measurement repeatability was similar to that achieved with NTA in this work (0.5-4%) and close to that reported by others in the literature (0.8-7.8 %) [33]. The EV peak areas exhibited a clear linear relationship ($R^2$ of 0.998) with the corresponding injected EV concentrations in the range of $2\times10^{11}$-$8\times10^{12}$ EVs/mL (Fig. 1-D). These results indicate that TDA-UV allows precise EV size measurement for concentrations ≥ $5\times10^{11}$ EVs/mL and can also be used for the determination of EV concentrations using a linear calibration curve established with standard EVs owing similar characteristics (i.e. origin, purity..).

To evaluate whether TDA is able to discriminate slight changes in EV size, we measured the size of an EV sample before and after incubation with a specific bovine anti-CD9 antibody, which is supposed to bind to CD9 tetraspanin, a membrane protein expressed on the surface of bovine milk-EVs [34]. This analysis was done on EVs isolated from frozen BM, pretreated by acid precipitation, using qEV70 column (f-BM-AP-qEV70). The mean size of EVs was found to increase from 210.1 ± 3.3 nm to 234.7 ± 25.4 nm after incubation of EVs with anti-CD9 antibodies (Fig. 2-A). A similar tendency was observed by NTA (Fig. 2-B). Even if values determined before and after incubation with the antibody did not significantly differ, the observed size increase is in accordance with the association of EVs with IgG monoclonal antibodies (~150 KDa) having a hydrodynamic size of ~10-13 nm [35–37]. This shows the accuracy of TDA and its capability to detect minor changes in EV sizes.

### 3.2. Application of TDA-UV to monitor the impact of isolation methods on EVs size

The developed and validated TDA-UV method was then employed to determine the sizes of different BM-derived EVs, prepared using different isolation protocols, in order to investigate the effect of pre-analytical variables (i.e. milk pretreatment and SEC columns used for their isolation) on the size heterogeneity and purity of extracted EVs.

#### 3.2.1. Impact of the freezing of bovine milk prior to EV isolation

First, we compared the sizes of EVs prepared from fresh BM (BM-AP-qEV35) or frozen BM (f-BM-AP-qEV35) but using same extraction protocol. The mean sizes determined by TDA for both EV samples were similar ($p$ >0.05), with values of 189.9 ± 5.4 nm and 194.0 ± 7.8 nm for EVs isolated from fresh and frozen BM, respectively (Fig. 3-A, Table 1). In both samples, the peak area corresponding to EVs represented more than 90 % of the total UV signal, while the remaining signal corresponded to residual small molecules of ~1 nm, which suggests similar low levels of protein contaminants, mainly β-lactoglobulin, within these samples. NTA analysis was in accordance with TDA showing no significant impact of the freezing of milk on the sizes of isolated EVs but did not point out the presence of protein contaminants (Fig. 3-A).

### 3.2.2. Impact of the type of SEC purification columns used to isolate EVs

The TDA-UV method was then used to evaluate the impact of the SEC purification columns on EV sizes. The mean size determined by TDA for EVs isolated from f-BM-AP using qEV70, of 210.1 ± 3.3 nm, was shown to be significantly higher ($p< 0.05$) than that obtained for EVs isolated using qEV35 column (194.0 ± 7.8 nm) (Fig. 3-A). However, the level of small contaminants (~1 nm) was similar (between 9 - 12%) in both samples (Table 1). Although qEV70 SEC column has an optimum recovery range shifted toward larger EVs (i.e. 70-1000 nm) compared to that of qEV35 (i.e. 35-350 nm), TDA showed only a slight increase of the mean EV size when isolated using qEV70. These results suggest that large EVs (> 350 nm) are rare in these samples and do not significantly influence the mean EV size when using qEV70 for their isolation. This can be explained by the 0.22 µm filtration step included in the EV isolation protocol (see section 2.2.1). Unlike TDA, NTA measurements showed no significant difference ($p> 0.05$) in EV sizes among the samples prepared using qEV70 (i.e. 172.0 ± 0.9 nm) or using qEV35 (i.e. 176.7 ± 7.0 nm) (Fig. 3-A, Table 1). This may be due to the important sample dilution required by NTA that could further minimize the influence of the low abundant large EVs on the measured average EV size.

### 3.2.3. Impact of the milk method used to discard the major milk proteins

The TDA-UV method was used to verify the purity of EV samples with different abundance of contaminating milk proteins. The EV sample obtained from milk pretreated by acid precipitation (f-BM-AP) using qEV70, was considered as sufficiently pure (88% of the total UV signal) (Fig. 3-B, Table 1). TDA measurements were then conducted on two samples obtained from f-BM that were pretreated mechanically using two different centrifugation

protocols (f-BM-C1 or C2), in order to discard the major milk proteins (caseins), prior to EV isolation from whey fractions using qEV70 column. Both samples were expected to exhibit higher protein contamination compared to the sample prepared by acid precipitation. This was evidenced by the 3 to 11-fold higher ratios of protein concentration/EV count measured by BCA assay and NTA for f-BM-C1 & C2, respectively. The Taylorgrams recorded from both samples showed an asymmetric broadening of the elution peaks (Fig. 3-B) resulting probably from the interaction between analytes within the sample and the capillary wall [38]. Furthermore, in agreement with the high ratios of protein to EVs determined for f-BM-C1 & C2, TDA analysis showed that molecular contaminants in both samples were very abundant (i.e. ~50 % and ~100 % of the total UV signal, respectively) compared to f-BM-AP (i.e. ~12%; Table 1). In addition, the average size of these contaminants was found higher in f-BM-C1 & C2 (2.8 and 12.7 nm, respectively) compared to f-BM-AP (1.1 nm). This is consistent with mass spectrometry analysis that showed abundance of various whey proteins (e.g. lactoferrin and bovine serum albumin), larger than β-lactoglobulin, in such samples (data not shown). TEM images were in excellent agreement with TDA showing the presence of more contaminant protein traces (electron dense smudges) in the samples isolated using centrifugation (Fig. 3-C), particularly in f-BM-C2 where EV imaging was hindered by the contaminants. The largest size population revealed by TDA in f-BM-C1 samples, which is attributed to EVs, showed a mean size of 95.4 ± 21.5 nm (Fig. 3-A), which is significantly smaller than that measured by TDA for EVs in f-BM-AP (i.e. 210.1 ± 3.3 nm). This can be explained by the presence of small sized protein aggregates, resulted from the aggregation propensity of the highly abundant proteins within the f-BM-C1 & C2 samples, that bias the analysis and lead to a shift of EV size toward smaller sizes.

### 3.2.4. EV size and purity in a WPC preparation

Finally, TDA analysis of EVs isolated from WPC using qEV70 SEC column showed a mean EV size of 121.5 $\pm$ 11.9 nm (Fig. 3-A), which contributed to ~91 % of the UV signal (Table 1). Small contaminants of 1.3 $\pm$ 0.4 nm were present at low proportion (i.e. ~9 %), similar to the results observed for EV samples isolated from BM treated by acid precipitation. However, compared to these latter, EVs isolated from WPC showed significantly smaller size as measured by TDA and NTA (Fig. 3-A, Table 1).

If most of the sizes determined for the different EV samples by TDA are relatively similar to those obtained by NTA, the results obtained from f-BM-C1 and f-BM-C2 samples, which exhibit high protein contamination, were particularly different between both techniques. These discrepancies arise from the difference in their working principles. NTA determines the Brownian motions of single particles, and subsequently their sizes, based on the light scattered by the particles, and thus has a restricted resolution for small particles and present a lower size limit of ~70 nm [33]. Thus, NTA is likely not influenced by the presence of high content of protein contaminants in the analyzed sample. In contrast, TDA determines the diffusion coefficient of analytes based on their dispersion under Poiseuille-like flow, allowing measurement of a wide range of sizes (from angstrom to submicrometer) [28]. These results show the potential of TDA as complementary technique allowing to evaluate the purity of EV samples by displaying the abundance of contaminating proteins. The purity (i.e. relative peak area of EVs among the total UV signal) of the different EV samples evaluated by TDA was repeatable (RSD of 0.3 - 6.7 %) for concentrations ≥ $5x10^{11}$ EVs/mL (Table 1).

### 3.3. TDA-LIF for monitoring the size of labeled EVs

The TDA method was then used with LIF detection to check whether we could use an alternative mode of detection. EVs were labeled with either CFDA-SE, an intravesicular dye, or through their surface markers, using an α-CD9 antibody conjugated to FITC.

TDA-LIF analysis of EVs labeled with CFDA-SE showed three subpopulations with mean sizes of 283.2 ± 33.5 nm, 38.0 ± 15.1 nm and 1.33 ± 0.03 nm, representing ~72 %, 13 % and 15 % of the total signal, respectively (Fig. 4). If the largest subpopulation (283.2 nm) corresponds to the labeled EVs, the one with a mean diameter of 38.0 nm is most likely very small EVs and/or fluorescent EV debris (i.e. conjugated to CFSE) that may result from the labeling process. The smallest size of 1.33 ± 0.03 nm represents the free dye that spontaneously hydrolyze and turn fluorescent. This was confirmed by TDA tests on free CFDA-SE (data not shown). To understand the size increase found for EVs after labeling with CFDA-SE (i.e. 283.2 ± 33.5 nm), compared to unlabeled EVs (i.e. 189 $\pm$ 5.4 nm, determined by TDA-UV), we applied the same washing protocol used to remove free CDFA to unlabeled EVs (centrifugation through a 30 kDa filter). We also observed a similar significant increase in the size of unlabeled EVs. This washing step is therefore responsible for that size increase

which may be due to EV aggregation and/or a tendency of the smallest EVs to adsorb onto the filter membrane.

The TDA-LIF detection was then used to evaluate the size of EVs labeled with anti-CD9 conjugated to FITC. Surprisingly, the size of labeled-EVs was found to be significantly smaller (163.6 ± 12.4 nm) than that determined by TDA-UV for the same EVs before labeling (189.9 ± 5.4 nm) (Fig. 4-B). This may be because TDA-LIF provide specific sizing of the EV subpopulation expressing CD9 tetraspanin. This latter protein marker was indeed found to be enriched in small EVs [39,40], which explains this shift toward smaller sizes measured by TDA despite the association of EVs with anti-CD9 antibodies. Furthermore, TDA revealed the presence of small contaminants of 5.8 ± 0.4 nm within the samples, suggesting the presence of residual FITC-conjugated antibodies and free FITC following EVs labeling.
TDA-LIF size measurements were also repeatable with RSDs in the range of 0.8-11.8 %. These results show the capacity of TDA-LIF to monitor the changes in EV size after different fluorescent labeling processes.

## 4. Conclusion

From our findings, we propose TDA as new method for the size characterization of heterogeneous EVs. TDA is an absolute method, requiring no size calibration, allowing to measure the hydrodynamic sizes of analytes within a small sample volume. This is of particular interest as the scientific community working on EVs is struggling to find relevant reference materials to calibrate and standardize EV analysis techniques. TDA could characterize the size of bovine milk-EVs, in their sample matrix, over their whole size range. Although TDA is capable to detect small EVs < 50 nm, which are below the lower limit of NTA, both techniques were shown to determine similar sizes at least for relatively low polydisperse and non-contaminated samples, such as bovine EVs used in our study.

Furthermore, TDA allows quantitative assessment of EVs and molecular contaminants (e.g. proteins) present in the samples. This makes TDA method very useful tool for the estimation of the purity of EV isolates (i.e. ratio of EVs to contaminating proteins), which is particularly important for subsequent use of EVs. Thus, TDA can be considered as a tool for simple, accurate and straightforward quality control of EV samples, which is currently addressed using approaches combining electron microscopy and western Blot that are labor intensive, time consuming, unsuited to routine daily use and lack accuracy [41]. Here, TDA was successfully applied to investigate the impact of pre-analytical variables on the

size heterogeneity and purity of isolated bovine EVs (Table 1). Our results showed that freezing of bovine milk prior to EV isolation seems to have no impact on the size of isolated EVs. On the other hand, the type of SEC purification column (qEV35 Vs qEV70) used in the isolation process had only a slight influence on the size of the resulting BM-derived EVs. Furthermore, acid precipitation was shown to be more efficient in removing milk proteins compared to centrifugation, resulting in EV preparations with significant higher purity.

Moreover, the TDA-LIF approach was shown to allow to monitor the changes in EV size after fluorescent labeling and also to distinguish EV sub-population based on their surface protein. This method has therefore a great potential to be used as a complementary approach for the size, quality characterization as well as the quantification of EVs. The integration of an online electrokinetic preconcentration of EVs in capillary at the forefront of TDA analysis, is currently being investigated in order to improve the sensitivity/LOD of this method.

**Table 1.** Summary of the results obtained by TDA and NTA on the different bovine milk-derived EV preparations. AP: acid precipitation; C1, C2: centrifugation protocols 1 or 2.

| | | | | | TDA | |
|---|---|---|---|---|---|---|
| **Sample** | **Frozen/fresh bovine milk** | **Protocol used to discard major milk proteins** | **SEC column** | **NTA (nm)** | **EV size (nm)** | **EV purity (Relative peak area of EVs among total UV signal)** |
| **BM-AP** | Fresh | AP | qEV35 | 178.7 ± 6.7 | 189.9 ± 5.4 | 94.3 ± 0.8 % |
| **f-BM-AP** | Frozen | AP | qEV35 | 176.7 ± 7.0 | 194.0 ± 7.8 | 91.1 ± 1.0 % |
| **f-BM-AP** | Frozen | AP | qEV70 | 172.0 ± 0.9 | 210.1 ± 3.3 | 88.0 ± 2.6 % |
| **f-BM-C1** | Frozen | C1 | qEV70 | 179.6 ± 0.7 | 95.4 ± 21.5 | 50.3 ± 2.0 % |
| **f-BM-C2** | Frozen | C2 | qEV70 | 179.2 ± 2.6 | * | < 50 % |
| **WPC** | Whey powder | AP | qEV70 | 146.1 ± 3.7 | 121.5 ± 11.9 | 91.1 ± 2.2 % |

(*) EV size determination was hindered by the high abundance of contaminants.

## Declaration of competing interest

The authors declare that they have no known competing financial interests or personal relationships that could have appeared to influence the work reported in this paper.

## CRediT authorship contribution statement

**Sameh Obeid:** Visualization, Methodology, Investigation, Data curation, Formal analysis, Writing – original draft. **Joseph Chamieh:** Data curation, Visualization, Writing - review & editing. **Thanh Duc Mai:** Conceptualization, Supervision, Visualization, Writing - review & editing. **Marco Morani:** Methodology, Preliminary investigation, Formal analysis. **Melissa Reyre:** Formal analysis, Data curation. **Zuzana Krupova:** Funding Acquisition, Investigation, Formal analysis, Data curation, Writing - review & editing**. Pierre Defrenaix:** Funding Acquisition, Project administration. **Hervé Cottet:** Data curation, Visualization, Writing - review & editing. **Myriam Taverna:** Conceptualization, Project administration, Funding Acquisition, Supervision, Validation, Writing - review & editing.

## Data availability

Data will be made available on request.

## Acknowledgements

This project was funded by “France Relance” (France recovery plan, contract 254315) and has received financial support from the Centre National de la Recherche Scientifique (CNRS) through the MITI program (Mission pour les Initiatives Transverses et Interdisciplinaires, 2021-2022). The authors thank Christine Longin, from University Paris-Saclay, INRAE, AgroParisTech, GABI (Jouy-en-Josas, France) for TEM imaging. We would like to thank Sophie Gallier, from the Dairy Goat Co-operative (N.Z.) (DGC, Ltd, Hamilton New Zealand) for providing the WPC samples.

## References


[1] N.S. Barteneva, E. Fasler-Kan, M. Bernimoulin, J.N.H. Stern, E.D. Ponomarev, L. Duckett, I.A. Vorobjev, Circulating microparticles: square the circle, BMC Cell Biol. 14 (2013) 23. https://doi.org/10.1186/1471-2121-14-23.

[2] T. Geng, P. Pan, E. Leung, Q. Chen, L. Chamley, Z. Wu, Recent Advancement and Technical Challenges in Developing Small Extracellular Vesicles for Cancer Drug Delivery, Pharm. Res. 38 (2021) 179–197. https://doi.org/10.1007/s11095-021-02988-z.

[3] G. van Niel, G. D'Angelo, G. Raposo, Shedding light on the cell biology of extracellular vesicles, Nat. Rev. Mol. Cell Biol. 19 (2018) 213–228. https://doi.org/10.1038/nrm.2017.125.

[4] C. Théry, K.W. Witwer, E. Aikawa, M.J. Alcaraz, J.D. Anderson, R. Andriantsitohaina, A. Antoniou, T. Arab, F. Archer, G.K. Atkin-Smith, D.C. Ayre, J.-M. Bach, D. Bachurski, H. Baharvand, L. Balaj, S. Baldacchino, N.N. Bauer, A.A. Baxter, M. Bebawy, C. Beckham, A. Bedina Zavec, A. Benmoussa, A.C. Berardi, P. Bergese, E. Bielska, C. Blenkiron, S. Bobis-Wozowicz, E. Boilard, W. Boireau, A. Bongiovanni, F.E. Borràs, S. Bosch, C.M. Boulanger, X. Breakefield, A.M. Breglio, M.Á. Brennan, D.R. Brigstock, A. Brisson, M.L. Broekman, J.F. Bromberg, P. Bryl-Górecka, S. Buch, A.H. Buck, D. Burger, S. Busatto, D. Buschmann, B. Bussolati, E.I. Buzás, J.B. Byrd, G. Camussi, D.R. Carter, S. Caruso, L.W. Chamley, Y.-T. Chang, C. Chen, S. Chen, L. Cheng, A.R. Chin, A. Clayton, S.P. Clerici, A. Cocks, E. Cocucci, R.J. Coffey, A. Cordeiro-da-Silva, Y. Couch, F.A. Coumans, B. Coyle, R. Crescitelli, M.F. Criado, C. D'Souza-Schorey, S. Das, A. Datta Chaudhuri, P. de Candia, E.F. De Santana, O. De Wever, H.A. del Portillo, T. Demaret, S. Deville, A. Devitt, B. Dhondt, D. Di Vizio, L.C. Dieterich, V. Dolo, A.P. Dominguez Rubio, M. Dominici, M.R. Dourado, T.A. Driedonks, F.V. Duarte, H.M. Duncan, R.M. Eichenberger, K. Ekström, S. EL Andaloussi, C. Elie-Caille, U. Erdbrügger, J.M. Falcón-Pérez, F. Fatima, J.E. Fish, M. Flores-Bellver, A. Försönits, A. Frelet-Barrand, F. Fricke, G. Fuhrmann, S. Gabrielsson, A. Gámez-Valero, C. Gardiner, K. Gärtner, R. Gaudin, Y.S. Gho, B. Giebel, C. Gilbert, M. Gimona, I. Giusti, D.C. Goberdhan, A. Görgens, S.M. Gorski, D.W. Greening, J.C. Gross, A. Gualerzi, G.N. Gupta, D. Gustafson, A. Handberg, R.A. Haraszti, P. Harrison, H. Hegyesi, A. Hendrix, A.F. Hill, F.H. Hochberg, K.F. Hoffmann, B. Holder, H. Holthofer, B. Hosseinkhani, G. Hu, Y. Huang, V. Huber, S. Hunt, A.G.-E. Ibrahim, T. Ikezu, J.M. Inal, M. Isin, A. Ivanova, H.K. Jackson, S. Jacobsen, S.M. Jay, M. Jayachandran, G. Jenster, L. Jiang, S.M. Johnson, J.C. Jones, A. Jong, T. Jovanovic-Talisman, S. Jung, R. Kalluri, S. Kano, S. Kaur, Y. Kawamura, E.T. Keller, D. Khamari, E. Khomyakova, A. Khvorova, P. Kierulf, K.P. Kim, T. Kislinger, M. Klingeborn, D.J. Klinke, M. Kornek, M.M. Kosanović, Á.F. Kovács, E.-M. Krämer-Albers, S. Krasemann, M. Krause, I.V. Kurochkin, G.D. Kusuma, S. Kuypers, S. Laitinen, S.M. Langevin, L.R. Languino, J. Lannigan, C. Lässer, L.C. Laurent, G. Lavieu, E. Lázaro-Ibáñez, S. Le Lay, M.-S. Lee, Y.X.F. Lee, D.S. Lemos, M. Lenassi, A. Leszczynska, I.T. Li, K. Liao, S.F. Libregts, E. Ligeti, R. Lim, S.K. Lim, A. Linē, K. Linnemannstöns, A. Llorente, C.A. Lombard, M.J. Lorenowicz, Á.M. Lörincz, J. Lötvall, J. Lovett, M.C. Lowry, X. Loyer, Q. Lu, B. Lukomska, T.R. Lunavat, S.L. Maas, H. Malhi, A. Marcilla, J. Mariani, J. Mariscal, E.S. Martens-Uzunova, L. Martin-Jaular, M.C. Martinez, V.R. Martins, M. Mathieu, S. Mathivanan, M. Maugeri, L.K. McGinnis, M.J. McVey, D.G. Meckes, K.L. Meehan, I. Mertens, V.R. Minciacchi, A. Möller, M. Møller Jørgensen, A. Morales-Kastresana, J. Morhayim, F. Mullier, M. Muraca, L. Musante, V. Mussack, D.C. Muth, K.H. Myburgh, T. Najrana, M. Nawaz, I. Nazarenko, P. Nejsum, C. Neri, T. Neri, R. Nieuwland, L. Nimrichter, J.P. Nolan, E.N. Nolte-'t Hoen, N. Noren Hooten, L. O'Driscoll, T. O'Grady, A.

O'Loghlen, T. Ochiya, M. Olivier, A. Ortiz, L.A. Ortiz, X. Osteikoetxea, O. Østergaard, M. Ostrowski, J. Park, D.M. Pegtel, H. Peinado, F. Perut, M.W. Pfaffl, D.G. Phinney, B.C. Pieters, R.C. Pink, D.S. Pisetsky, E. Pogge von Strandmann, I. Polakovicova, I.K. Poon, B.H. Powell, I. Prada, L. Pulliam, P. Quesenberry, A. Radeghieri, R.L. Raffai, S. Raimondo, J. Rak, M.I. Ramirez, G. Raposo, M.S. Rayyan, N. Regev-Rudzki, F.L. Ricklefs, P.D. Robbins, D.D. Roberts, S.C. Rodrigues, E. Rohde, S. Rome, K.M. Rouschop, A. Rughetti, A.E. Russell, P. Saá, S. Sahoo, E. Salas-Huenuleo, C. Sánchez, J.A. Saugstad, M.J. Saul, R.M. Schiffelers, R. Schneider, T.H. Schøyen, A. Scott, E. Shahaj, S. Sharma, O. Shatnyeva, F. Shekari, G.V. Shelke, A.K. Shetty, K. Shiba, P.R.-M. Siljander, A.M. Silva, A. Skowronek, O.L. Snyder, R.P. Soares, B.W. Sódar, C. Soekmadji, J. Sotillo, P.D. Stahl, W. Stoorvogel, S.L. Stott, E.F. Strasser, S. Swift, H. Tahara, M. Tewari, K. Timms, S. Tiwari, R. Tixeira, M. Tkach, W.S. Toh, R. Tomasini, A.C. Torrecilhas, J.P. Tosar, V. Toxavidis, L. Urbanelli, P. Vader, B.W. van Balkom, S.G. van der Grein, J. Van Deun, M.J. van Herwijnen, K. Van Keuren-Jensen, G. van Niel, M.E. van Royen, A.J. van Wijnen, M.H. Vasconcelos, I.J. Vechetti, T.D. Veit, L.J. Vella, É. Velot, F.J. Verweij, B. Vestad, J.L. Viñas, T. Visnovitz, K.V. Vukman, J. Wahlgren, D.C. Watson, M.H. Wauben, A. Weaver, J.P. Webber, V. Weber, A.M. Wehman, D.J. Weiss, J.A. Welsh, S. Wendt, A.M. Wheelock, Z. Wiener, L. Witte, J. Wolfram, A. Xagorari, P. Xander, J. Xu, X. Yan, M. Yáñez-Mó, H. Yin, Y. Yuana, V. Zappulli, J. Zarubova, V. Žėkas, J. Zhang, Z. Zhao, L. Zheng, A.R. Zheutlin, A.M. Zickler, P. Zimmermann, A.M. Zivkovic, D. Zocco, E.K. Zuba-Surma, Minimal information for studies of extracellular vesicles 2018 (MISEV2018): a position statement of the International Society for Extracellular Vesicles and update of the MISEV2014 guidelines, J. Extracell. Vesicles. 7 (2018) 1535750. https://doi.org/10.1080/20013078.2018.1535750.

[5] M. Colombo, G. Raposo, C. Théry, Biogenesis, secretion, and intercellular interactions of exosomes and other extracellular vesicles, Annu. Rev. Cell Dev. Biol. 30 (2014) 255–289. https://doi.org/10.1146/annurev-cellbio-101512-122326.

[6] I.K. Herrmann, M.J.A. Wood, G. Fuhrmann, Extracellular vesicles as a next-generation drug delivery platform, Nat. Nanotechnol. 16 (2021) 748–759. https://doi.org/10.1038/s41565-021-00931-2.

[7] C. Gardiner, D. Di Vizio, S. Sahoo, C. Théry, K.W. Witwer, M. Wauben, A.F. Hill, Techniques used for the isolation and characterization of extracellular vesicles: results of a worldwide survey, J. Extracell. Vesicles. 5 (2016) 32945. https://doi.org/10.3402/jev.v5.32945.

[8] H. Shao, H. Im, C.M. Castro, X. Breakefield, R. Weissleder, H. Lee, New Technologies for Analysis of Extracellular Vesicles, Chem. Rev. 118 (2018) 1917–1950. https://doi.org/10.1021/acs.chemrev.7b00534.

[9] S. Tiwari, V. Kumar, S. Randhawa, S.K. Verma, Preparation and characterization of extracellular vesicles, Am. J. Reprod. Immunol. 85 (2021) e13367. https://doi.org/10.1111/aji.13367.

[10] S.H. Hilton, I.M. White, Advances in the analysis of single extracellular vesicles: A critical review, Sens. Actuators Rep. 3 (2021) 100052. https://doi.org/10.1016/j.snr.2021.100052.

[11] M. Havers, A. Broman, A. Lenshof, T. Laurell, Advancement and obstacles in microfluidics-based isolation of extracellular vesicles, Anal. Bioanal. Chem. (2022). https://doi.org/10.1007/s00216-022-04362-3.

[12] M.I. Ramirez, M.G. Amorim, C. Gadelha, I. Milic, J.A. Welsh, V.M. Freitas, M. Nawaz, N. Akbar, Y. Couch, L. Makin, F. Cooke, A.L. Vettore, P.X. Batista, R. Freezor, J.A. Pezuk, L. Rosa-Fernandes, A.C.O. Carreira, A. Devitt, L. Jacobs, I.T. Silva, G. Coakley, D.N. Nunes, D. Carter, G. Palmisano, E. Dias-Neto, Technical challenges of working with extracellular vesicles, Nanoscale. 10 (2018) 881–906. https://doi.org/10.1039/c7nr08360b.
[13] J. Stam, S. Bartel, R. Bischoff, J.C. Wolters, Isolation of extracellular vesicles with combined enrichment methods, J. Chromatogr. B. 1169 (2021) 122604. https://doi.org/10.1016/j.jchromb.2021.122604.
[14] W. Phillips, E. Willms, A.F. Hill, Understanding extracellular vesicle and nanoparticle heterogeneity: Novel methods and considerations, PROTEOMICS. 21 (2021) 2000118. https://doi.org/10.1002/pmic.202000118.
[15] Y. Couch, E.I. Buzàs, D. Di Vizio, Y.S. Gho, P. Harrison, A.F. Hill, J. Lötvall, G. Raposo, P.D. Stahl, C. Théry, K.W. Witwer, D.R.F. Carter, A brief history of nearly EV-erything – The rise and rise of extracellular vesicles, J. Extracell. Vesicles. 10 (2021) e12144. https://doi.org/10.1002/jev2.12144.
[16] J.A. Welsh, E. van der Pol, B.A. Bettin, D.R.F. Carter, A. Hendrix, M. Lenassi, M.-A. Langlois, A. Llorente, A.S. van de Nes, R. Nieuwland, V. Tang, L. Wang, K.W. Witwer, J.C. Jones, Towards defining reference materials for measuring extracellular vesicle refractive index, epitope abundance, size and concentration, J. Extracell. Vesicles. 9 (2020) 1816641. https://doi.org/10.1080/20013078.2020.1816641.
[17] G.I. Taylor, Dispersion of soluble matter in solvent flowing slowly through a tube, Proc. R. Soc. Lond. Ser. Math. Phys. Sci. 219 (1953) 186–203. https://doi.org/10.1098/rspa.1953.0139.
[18] M.R. Moser, C.A. Baker, Taylor dispersion analysis in fused silica capillaries: a tutorial review, Anal. Methods. 13 (2021) 2357–2373. https://doi.org/10.1039/D1AY00588J.
[19] C. Malburet, L. Leclercq, J.-F. Cotte, J. Thiebaud, E. Bazin, M. Garinot, H. Cottet, Taylor Dispersion Analysis to support lipid-nanoparticle formulations for mRNA vaccines, Gene Ther. (2022) 1–8. https://doi.org/10.1038/s41434-022-00370-1.
[20] L. Labied, P. Rocchi, T. Doussineau, J. Randon, O. Tillement, F. Lux, A. Hagège, Taylor Dispersion Analysis Coupled to Inductively Coupled Plasma-Mass Spectrometry for Ultrasmall Nanoparticle Size Measurement: From Drug Product to Biological Media Studies, Anal. Chem. 93 (2021) 1254–1259. https://doi.org/10.1021/acs.analchem.0c03988.
[21] L. Leclercq, P. Saetear, A. Rolland-Sabaté, J.-P. Biron, J. Chamieh, L. Cipelletti, D.J. Bornhop, H. Cottet, Size-Based Characterization of Polysaccharides by Taylor Dispersion Analysis with Photochemical Oxidation or Backscattering Interferometry Detections, Macromolecules. 52 (2019) 4421–4431. https://doi.org/10.1021/acs.macromol.9b00605.
[22] U.B. Høgstedt, G. Schwach, M. van de Weert, J. Østergaard, Taylor Dispersion Analysis as a promising tool for assessment of peptide-peptide interactions, Eur. J. Pharm. Sci. 93 (2016) 21–28. https://doi.org/10.1016/j.ejps.2016.07.015.
[23] W. Hulse, R. Forbes, A Taylor dispersion analysis method for the sizing of therapeutic proteins and their aggregates using nanolitre sample quantities, Int. J. Pharm. 416 (2011) 394–397. https://doi.org/10.1016/j.ijpharm.2011.06.045.
[24] J. Chamieh, H. Merdassi, J.-C. Rossi, V. Jannin, F. Demarne, H. Cottet, Size characterization of lipid-based self-emulsifying pharmaceutical excipients during

lipolysis using Taylor dispersion analysis with fluorescence detection, Int. J. Pharm. 537 (2018) 94–101. https://doi.org/10.1016/j.ijpharm.2017.12.032.
[25] J. Chamieh, F. Davanier, V. Jannin, F. Demarne, H. Cottet, Size characterization of commercial micelles and microemulsions by Taylor dispersion analysis, Int. J. Pharm. 492 (2015) 46–54. https://doi.org/10.1016/j.ijpharm.2015.06.037.
[26] U. Franzen, C. Vermehren, H. Jensen, J. Østergaard, Physicochemical characterization of a PEGylated liposomal drug formulation using capillary electrophoresis, ELECTROPHORESIS. 32 (2011) 738–748. https://doi.org/10.1002/elps.201000552.
[27] C. Malburet, L. Leclercq, J.-F. Cotte, J. Thiebaud, E. Bazin, M. Garinot, H. Cottet, Size and Charge Characterization of Lipid Nanoparticles for mRNA Vaccines, Anal. Chem. 94 (2022) 4677–4685. https://doi.org/10.1021/acs.analchem.1c04778.
[28] J. Chamieh, L. Leclercq, M. Martin, S. Slaoui, H. Jensen, J. Østergaard, H. Cottet, Limits in Size of Taylor Dispersion Analysis: Representation of the Different Hydrodynamic Regimes and Application to the Size-Characterization of Cubosomes, Anal. Chem. 89 (2017) 13487–13493. https://doi.org/10.1021/acs.analchem.7b03806.
[29] H. Cottet, J.-P. Biron, M. Martin, On the optimization of operating conditions for Taylor dispersion analysis of mixtures, Analyst. 139 (2014) 3552–3562. https://doi.org/10.1039/C4AN00192C.
[30] G. Taylor, Conditions under Which Dispersion of a Solute in a Stream of Solvent can be Used to Measure Molecular Diffusion, Proc. R. Soc. Lond. Ser. A. 225 (1954) 473–477. https://doi.org/10.1098/rspa.1954.0216.
[31] M. Morani, T.D. Mai, Z. Krupova, P. Defrenaix, E. Multia, M.-L. Riekkola, M. Taverna, Electrokinetic characterization of extracellular vesicles with capillary electrophoresis: A new tool for their identification and quantification, Anal. Chim. Acta. 1128 (2020) 42–51. https://doi.org/10.1016/j.aca.2020.06.073.
[32] S. Ma, X. Yang, C. Zhao, M. Guo, Ultrasound-induced changes in structural and physicochemical properties of β-lactoglobulin, Food Sci. Nutr. 6 (2018) 1053–1064. https://doi.org/10.1002/fsn3.646.
[33] D. Bachurski, M. Schuldner, P.-H. Nguyen, A. Malz, K.S. Reiners, P.C. Grenzi, F. Babatz, A.C. Schauss, H.P. Hansen, M. Hallek, E. Pogge von Strandmann, Extracellular vesicle measurements with nanoparticle tracking analysis - An accuracy and repeatability comparison between NanoSight NS300 and ZetaView, J. Extracell. Vesicles. 8 (2019) 1596016. https://doi.org/10.1080/20013078.2019.1596016.
[34] M. Samuel, D. Chisanga, M. Liem, S. Keerthikumar, S. Anand, C.-S. Ang, C.G. Adda, E. Versteegen, M. Jois, S. Mathivanan, Bovine milk-derived exosomes from colostrum are enriched with proteins implicated in immune response and growth, Sci. Rep. 7 (2017) 5933. https://doi.org/10.1038/s41598-017-06288-8.
[35] A. Hawe, W.L. Hulse, W. Jiskoot, R.T. Forbes, Taylor Dispersion Analysis Compared to Dynamic Light Scattering for the Size Analysis of Therapeutic Peptides and Proteins and Their Aggregates, Pharm. Res. 28 (2011) 2302–2310. https://doi.org/10.1007/s11095-011-0460-3.
[36] A. Hawe, W. Friess, M. Sutter, W. Jiskoot, Online fluorescent dye detection method for the characterization of immunoglobulin G aggregation by size exclusion chromatography and asymmetrical flow field flow fractionation, Anal. Biochem. 378 (2008) 115–122. https://doi.org/10.1016/j.ab.2008.03.050.

[37] H. Zhao, O. Graf, N. Milovic, X. Luan, M. Bluemel, M. Smolny, K. Forrer, Formulation development of antibodies using robotic system and high-throughput laboratory (HTL), J. Pharm. Sci. 99 (2010) 2279–2294. https://doi.org/10.1002/jps.22008.
[38] S. Latunde-Dada, R. Bott, K. Hampton, O.I. Leszczyszyn, Analytical mitigation of solute–capillary interactions in double detection Taylor Dispersion Analysis, J. Chromatogr. A. 1408 (2015) 255–260. https://doi.org/10.1016/j.chroma.2015.07.015.
[39] D.K. Jeppesen, A.M. Fenix, J.L. Franklin, J.N. Higginbotham, Q. Zhang, L.J. Zimmerman, D.C. Liebler, J. Ping, Q. Liu, R. Evans, W.H. Fissell, J.G. Patton, L.H. Rome, D.T. Burnette, R.J. Coffey, Reassessment of Exosome Composition, Cell. 177 (2019) 428-445.e18. https://doi.org/10.1016/j.cell.2019.02.029.
[40] J. Kowal, G. Arras, M. Colombo, M. Jouve, J.P. Morath, B. Primdal-Bengtson, F. Dingli, D. Loew, M. Tkach, C. Théry, Proteomic comparison defines novel markers to characterize heterogeneous populations of extracellular vesicle subtypes, Proc. Natl. Acad. Sci. U. S. A. 113 (2016) E968-977. https://doi.org/10.1073/pnas.1521230113.
[41] J. Webber, A. Clayton, How pure are your vesicles?, J. Extracell. Vesicles. 2 (2013) 19861. https://doi.org/10.3402/jev.v2i0.19861.

## Figure captions

***Fig. 1.*** *Size characterization by TDA (A, C, D) or by NTA (B) of EVs isolated from fresh BM-AP using qEVoriginal SEC 35 nm column. (A) Taylorgrams representing three repetitions obtained by injecting EVs at 2x10$^{12}$ EVs/mL. Two-Gaussian fit shown in dotted black line, was required due to the presence of small contaminants within the sample appearing as small peak on the top of the signal corresponding to EVs. Taylorgrams were aligned on the $x$-scale for better visual comparison. (B) NTA profile with the average EV size obtained. (C) TDA measurement repeatability determined at different EV injected concentrations. (D) Mean peak area, corresponding to EV contribution, plotted as function of injected EV concentration. Data represent mean ± SD of triplicate measurements. BM: bovine milk; AP: acid precipitation.*

**Fig. 2.** Size characterization obtained by TDA (A) or NTA (B) for EVs before and after incubation with specific α-CD9 antibody. EVs were isolated from f-BM-AP using qEVoriginal SEC 70 nm. Data represent mean ± SD of triplicate measurements. f-BM: frozen bovine milk; AP: acid precipitation. Taylorgrams in (A) were aligned on the *x*-scale for better visual comparison.

***Fig. 3.*** *Size measured using TDA or NTA for the different BM-derived EV samples prepared using different protocols (A). All TDA analyses were performed by injecting EVs at 2x10$^{12}$ EVs/mL. Data represent mean ± SD of triplicate measurements. (B) Representative Taylorgrams and (C) TEM images of EVs isolated from frozen bovine milk (f-BM), pretreated either by acid precipitation (AP) or by two different centrifugation protocols (i.e. C1 or C2), using qEV70 SEC column. White arrows indicate EVs. High electron-dense -black- patches in TEM micrographs correspond to protein dense regions. Taylorgrams in (B) were aligned on the $x$-scale for better visual comparison.*

***Fig. 4.*** *TDA-LIF of fluorescently labeled EVs. (A) Taylorgrams obtained from EVs labeled by CFDA-SE or anti-CD9 conjugated to FITC. EVs were isolated from fresh BM-AP using qEVoriginal SEC 35 nm column prior to labeling. Taylorgrams were aligned on the $x$-scale for better visual comparison. (B) EV hydrodynamic diameter obtained by TDA-UV, for unlabeled EVs, or by TDA-LIF for fluorescently labeled-EVs. Data represent mean ± SD of triplicate measurements.*

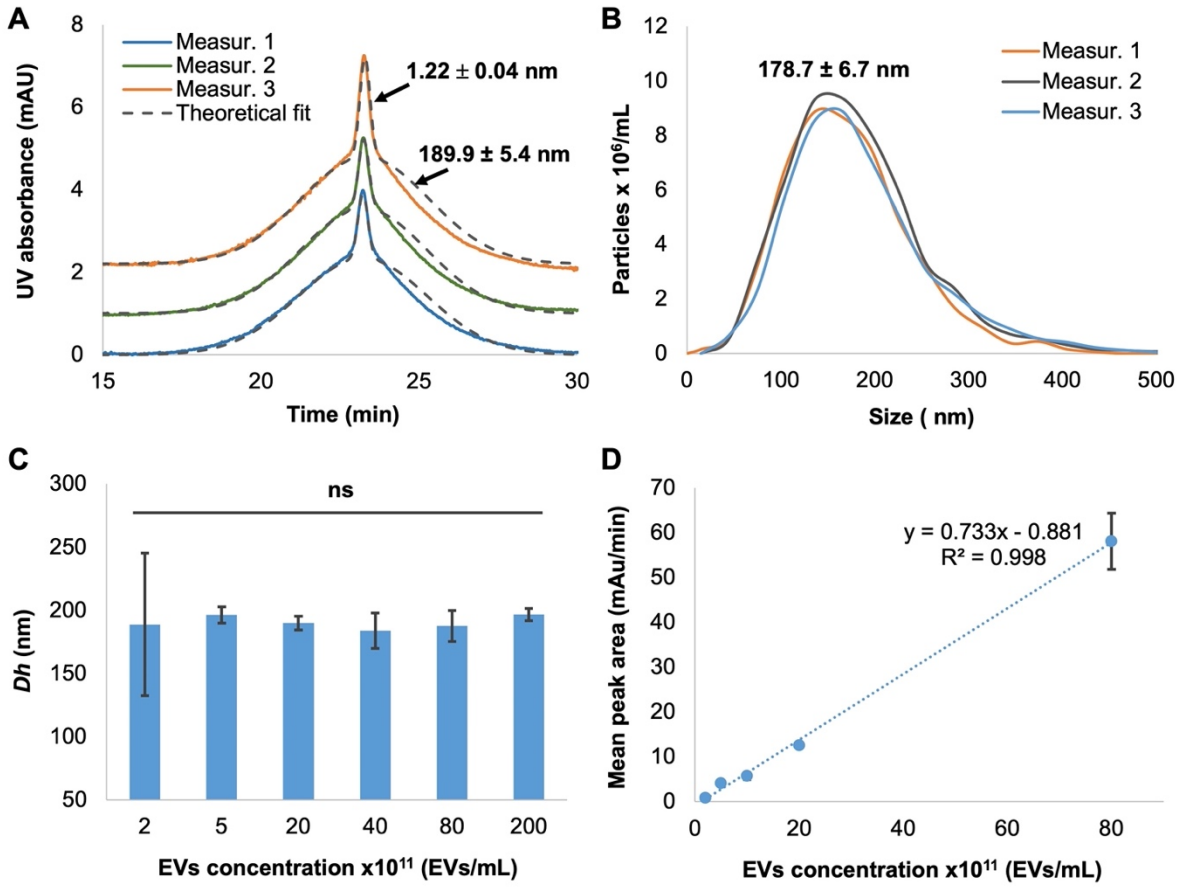
A
Measur. 1
Measur. 2
Measur. 3
Theoretical fit
1.22 ± 0.04 nm
189.9 ± 5.4 nm
UV absorbance (mAU)
Time (min)
B
178.7 ± 6.7 nm
Measur. 1
Measur. 2
Measur. 3
Particles x 10⁶/mL
Size ( nm)
C
ns
Dh (nm)
EVs concentration x10¹¹ (EVs/mL)
D
y = 0.733x - 0.881
R² = 0.998
Mean peak area (mAu/min)
EVs concentration x10¹¹ (EVs/mL)

Fig.1

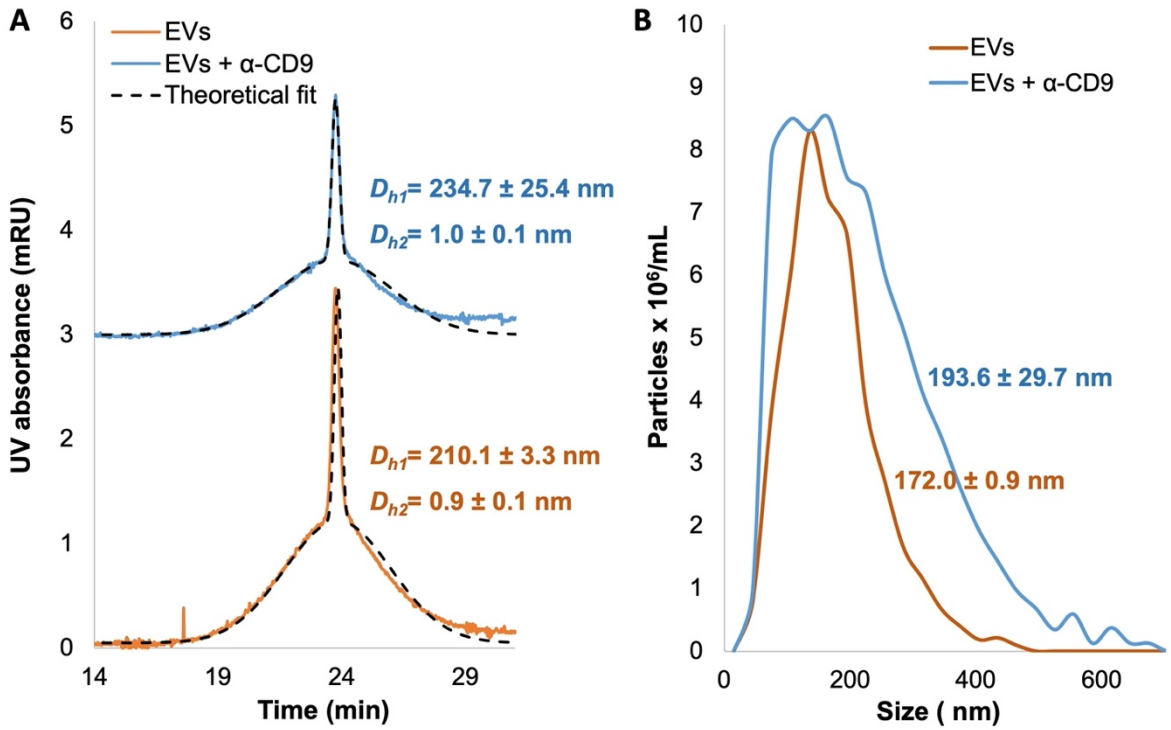
A
EVs
EVs + α-CD9
Theoretical fit
$D_{h1}$= 234.7 ± 25.4 nm
$D_{h2}$= 1.0 ± 0.1 nm
$D_{h1}$= 210.1 ± 3.3 nm
$D_{h2}$= 0.9 ± 0.1 nm
UV absorbance (mRU)
Time (min)
B
EVs
EVs + α-CD9
193.6 ± 29.7 nm
172.0 ± 0.9 nm
Particles x 10⁶/mL
Size ( nm)

Fig.2

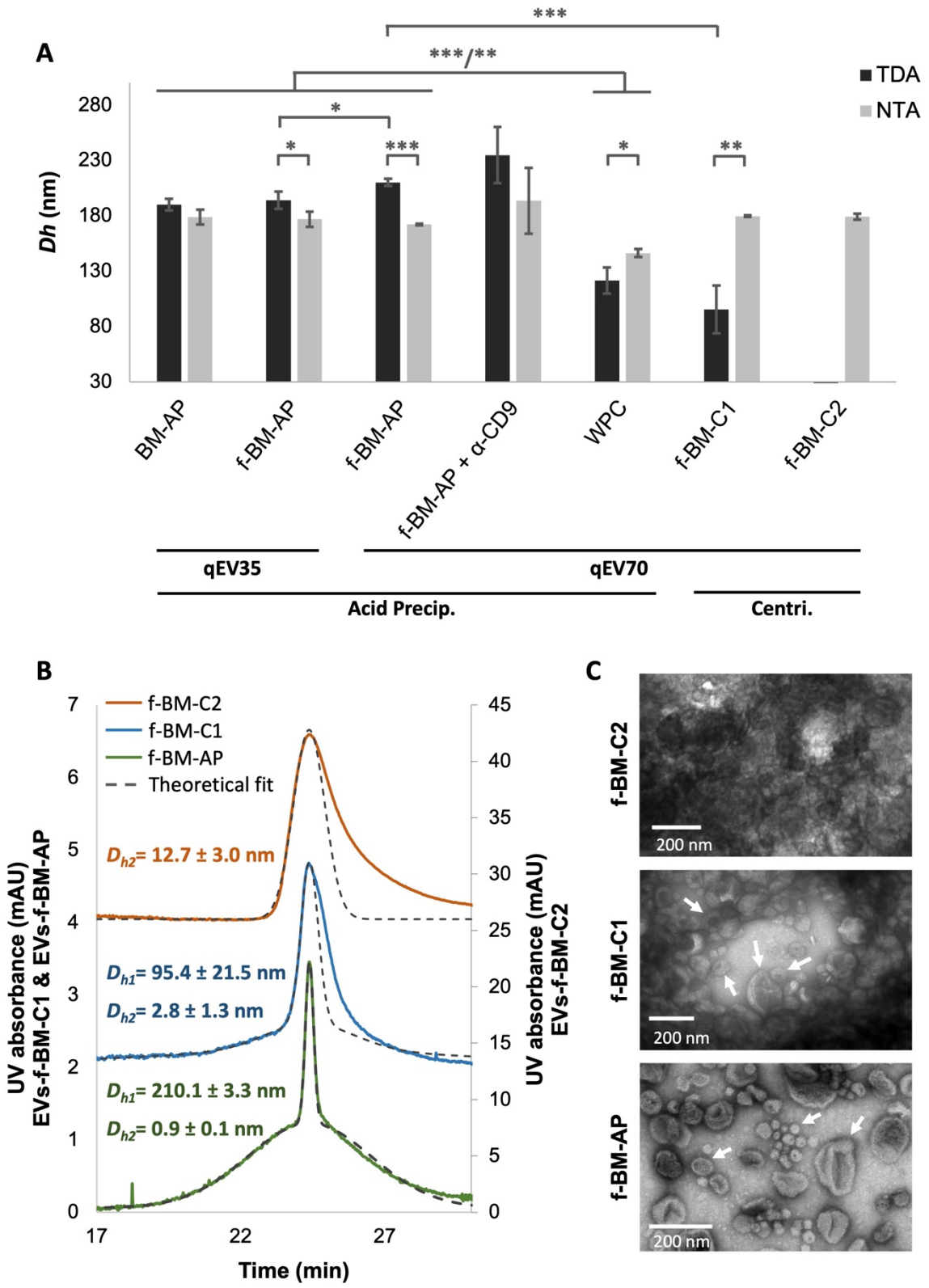
A
***
***/**
*
*
***
*
**
TDA
NTA
Dh (nm)
280
230
180
130
80
30
BM-AP
f-BM-AP
f-BM-AP
f-BM-AP + α-CD9
WPC
f-BM-C1
f-BM-C2
qEV35
qEV70
Acid Precip.
Centri.
B
f-BM-C2
f-BM-C1
f-BM-AP
Theoretical fit
$D_{h2}$= 12.7 ± 3.0 nm
$D_{h1}$= 95.4 ± 21.5 nm
$D_{h2}$= 2.8 ± 1.3 nm
$D_{h1}$= 210.1 ± 3.3 nm
$D_{h2}$= 0.9 ± 0.1 nm
UV absorbance (mAU)
EVs-f-BM-C1 & EVs-f-BM-AP
UV absorbance (mAU)
EVs-f-BM-C2
Time (min)
C
f-BM-C2
f-BM-C1
f-BM-AP
200 nm

Fig.3

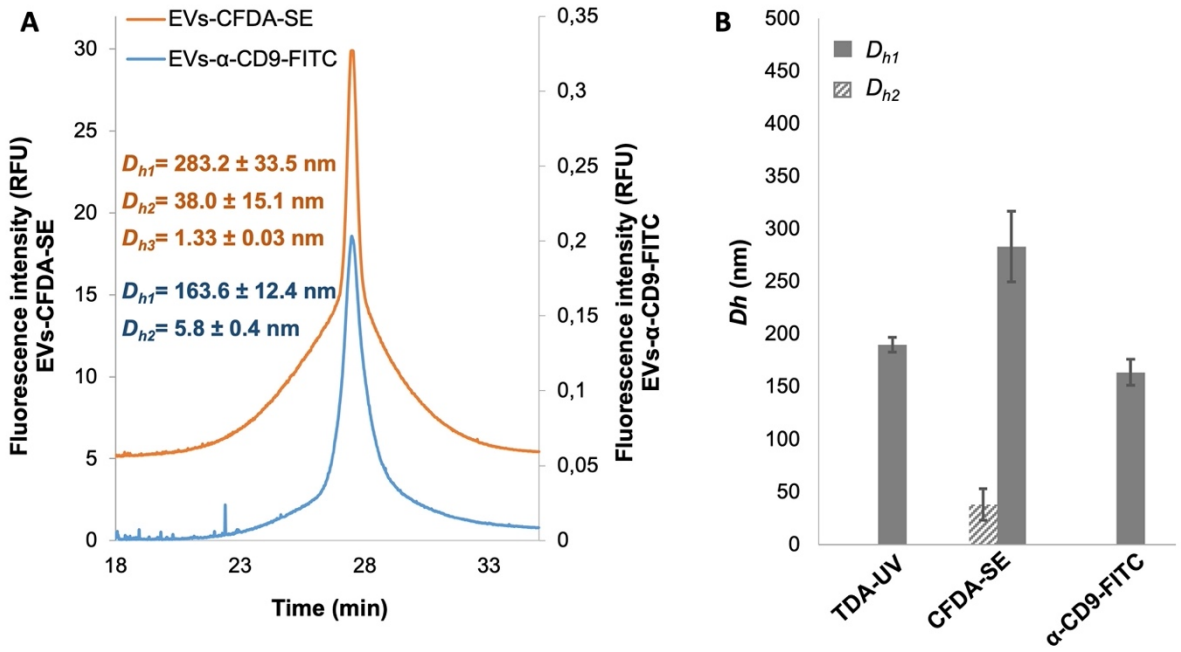
A
EVs-CFDA-SE
EVs-α-CD9-FITC
$D_{h1}$= 283.2 ± 33.5 nm
$D_{h2}$= 38.0 ± 15.1 nm
$D_{h3}$= 1.33 ± 0.03 nm
$D_{h1}$= 163.6 ± 12.4 nm
$D_{h2}$= 5.8 ± 0.4 nm
Fluorescence intensity (RFU) EVs-CFDA-SE
Fluorescence intensity (RFU) EVs-α-CD9-FITC
Time (min)
B
$D_{h1}$
$D_{h2}$
Dh (nm)
TDA-UV
CFDA-SE
α-CD9-FITC

Fig.4